

## Strong enhancement of superconductivity at high pressures within the charge-density-wave states of $2H$ -TaS<sub>2</sub> and $2H$ -TaSe<sub>2</sub>

D. C. Freitas,<sup>1,2,3</sup> P. Rodière,<sup>1,2</sup> M. R. Osorio,<sup>4</sup> E. Navarro-Moratalla,<sup>5</sup> N. M. Nemes,<sup>6</sup> V. G. Tissen,<sup>4,7,\*</sup> L. Cario,<sup>8</sup> E. Coronado,<sup>5</sup> M. García-Hernández,<sup>9,10</sup> S. Vieira,<sup>4,10</sup> M. Núñez-Regueiro,<sup>1,2,†</sup> and H. Suderow<sup>4,10</sup>

<sup>1</sup>Université Grenoble Alpes, Institut Néel, F-38000 Grenoble, France

<sup>2</sup>CNRS, Institut Néel, F-38000 Grenoble, France

<sup>3</sup>Centro Brasileiro de Pesquisas Físicas, Rua Dr. Xavier Sigaud, 150, Urca, Rio de Janeiro–RJ, Brazil

<sup>4</sup>Laboratorio de Bajas Temperaturas, Departamento de Física de la Materia Condensada, Instituto de Ciencia de Materiales Nicolás Cabrera, Condensed Matter Physics Center (IFIMAC), Universidad Autónoma de Madrid, E-28049 Madrid, Spain

<sup>5</sup>Instituto de Ciencia Molecular (ICMol), Universidad de Valencia, Catedrático José Beltrán 2, E-46980 Paterna, Spain

<sup>6</sup>GFMC, Departamento de Física Aplicada III, Universidad Complutense de Madrid, Campus Moncloa, E-28040 Madrid, Spain

<sup>7</sup>Institute of Solid State Physics, Chernogolovka, 142432 Moscow Region, Russia

<sup>8</sup>Institut des Matériaux Jean Rouxel (IMN), Université de Nantes, CNRS, 2 rue de la Houssinière, BP 32229, F-44322 Nantes Cedex 03, France

<sup>9</sup>Instituto de Ciencia de Materiales de Madrid-CSIC, Cantoblanco E-28049 Madrid, Spain

<sup>10</sup>Unidad Asociada de Bajas Temperaturas y Altos Campos Magnéticos, UAM, CSIC, Madrid, Spain

(Received 21 October 2015; revised manuscript received 30 March 2016; published 24 May 2016)

We present measurements of the superconducting and charge-density-wave (CDW) critical temperatures ( $T_c$  and  $T_{CDW}$ ) as a function of pressure in the transition metal dichalcogenides  $2H$ -TaSe<sub>2</sub> and  $2H$ -TaS<sub>2</sub>. Resistance and susceptibility measurements show that  $T_c$  increases from temperatures below 1 K up to 8.5 K at 9.5 GPa in  $2H$ -TaS<sub>2</sub> and 8.2 K at 23 GPa in  $2H$ -TaSe<sub>2</sub>. We observe a kink in the pressure dependence of  $T_{CDW}$  at about 4 GPa that we attribute to the lock-in transition from incommensurate CDW to commensurate CDW. Above this pressure, the commensurate  $T_{CDW}$  slowly decreases, coexisting with superconductivity within our full pressure range.

DOI: [10.1103/PhysRevB.93.184512](https://doi.org/10.1103/PhysRevB.93.184512)

### I. INTRODUCTION

The near absence of reports on superconductivity in graphene and related single-layer systems is notorious, given the large efforts devoted presently to these materials. Only recently have superconducting signatures in doped graphene sheets [1,2] and Ising superconductivity in trigonal prismatic monolayer MoS<sub>2</sub> [3,4] and NbSe<sub>2</sub> [5] been observed. Few-layer devices have been also made of transition metal dichalcogenides ( $2H$ - $TX_2$ , with  $T = \text{Nb, Ta}$  and  $X = \text{S, Se}$ ), which crystallize in a hexagonal arrangement of transition metal atoms separated by the chalcogen. Single molecular layers, formed by hexagonal  $T$ - $X$  groups, show opposing tendencies with decreasing thickness—a reduction of superconducting  $T_c$  in  $2H$ -NbSe<sub>2</sub> and an increase in  $2H$ -TaS<sub>2</sub> [6–10].

Layered materials are generally very sensitive to modifications of their lattice parameters [11–19]. To understand their superconducting  $T_c$ , we need to address the interplay between superconductivity and the charge density wave (CDW) and how this interplay evolves when varying the lattice parameters.

It has been argued [11,20] that superconductivity and CDW strongly interact in  $2H$ - $TX_2$ . Initial discussions pointed out that there was a mutually exclusive interaction. Indeed,  $T_c$  decreases and  $T_{CDW}$  increases when the lattice parameter  $a/c$  ratio decreases as we pass from  $2H$ -NbS<sub>2</sub> ( $T_c = 6$  K and  $T_{CDW} = 0$  K),  $2H$ -NbSe<sub>2</sub> ( $T_c = 7.2$  K and  $T_{CDW} = 30$  K),  $2H$ -TaS<sub>2</sub> ( $T_c = 1$  K and  $T_{CDW} = 80$  K), and  $2H$ -TaSe<sub>2</sub>

( $T_c = 0.1$  K and  $T_{CDW} = 120$  K). On application of pressure in  $2H$ -NbSe<sub>2</sub>, the CDW disappears above 5 GPa and  $T_c$  increases slightly up to 8.5 K at 10 GPa [12,18], pointing out an exclusive interaction, too. Measurements of the superconducting density of states and of vortex core shapes in  $2H$ -NbSe<sub>2</sub> show that the superconducting gap of  $2H$ -NbSe<sub>2</sub> is strongly shaped by the CDW, and it has been argued that the CDW decreases the gap value along certain directions in real space [21]. Angular resolved photoemission also shows interesting correlations between superconducting and CDW Fermi-surface features. If these are cooperative or exclusive is, however, not clearly established when taking different photoemission measurements into account [22,23]. Thus, most experiments point out that, particularly from data in  $2H$ -NbSe<sub>2</sub>, the interaction seems to be of a competing nature. The mutual interaction between superconductivity and magnetism is debated in the cuprate compounds, where cooperative interactions have been discussed [24]. Here we find that, unexpectedly, CDW and superconductivity coexist in a large part of the phase diagram when applying pressure to the Ta-based  $2H$ - $TX_2$ , namely,  $2H$ -TaS<sub>2</sub> and  $2H$ -TaSe<sub>2</sub>.

In compounds with the largest interlayer separation and highest CDW transition temperatures,  $2H$ -TaS<sub>2</sub> and  $2H$ -TaSe<sub>2</sub>, the CDW and superconducting phase diagrams have been studied up to 4 GPa. The superconducting  $T_c$  increases in both compounds, up to about 2.5 K in  $2H$ -TaS<sub>2</sub> and 0.4 K in  $2H$ -TaSe<sub>2</sub> [25]. In  $2H$ -TaS<sub>2</sub>, the resistivity versus temperature curve as a function of pressure shows that the CDW appearing below 80 K at ambient pressure decreases down to about 66 K at 3.5 GPa in  $2H$ -TaS<sub>2</sub> [11,26,27]. In  $2H$ -TaSe<sub>2</sub>, the ambient pressure phase diagram consists of

\*Deceased.

†Corresponding author: [nunez@neel.cnrs.fr](mailto:nunez@neel.cnrs.fr)

an incommensurate CDW (ICDW) appearing at 120 K and a lock-in transition at 90 K to a commensurate CDW (CCDW). There is a reentrant lock-in transition with pressure [28]. The incommensurate CDW occupies the whole temperature range above 2 GPa, but, above 4 GPa, it locks to the lattice and again becomes commensurate [28–33]. Here we study the effect of pressure up to 25 GPa on superconductivity and charge density waves in  $2H$ -TaS<sub>2</sub> and  $2H$ -TaSe<sub>2</sub>. We find that the CDW does not disappear up to the highest pressures studied and that  $T_c$  increases considerably up to close to 9 K in both compounds.

## II. EXPERIMENT

To make a comparative study of both  $T_{CDW}$  and  $T_c$  under pressure we measure the magnetic susceptibility and the resistivity of small samples. The samples were grown using vapor transport and the polytype purity of the  $2H$  phase was checked by powder x-ray diffraction [26]. To this end, samples of synthesized crystals were ground and loaded inside a capillary ready for powder x-ray diffraction (performed in ambient conditions). Indexation of the reflections of the powder pattern by assuming a hexagonal symmetry allowed for the identification of a single phase with the following unit cell parameters:  $a = b = 3.3137(2)$  Å,  $c = 12.076(1)$  Å for  $2H$ -TaS<sub>2</sub> and  $a = b = 3.43910(5)$  Å,  $c = 12.7067(2)$  Å for  $2H$ -TaSe<sub>2</sub>. The Le Bail refinement of the room temperature powder pattern is in agreement with that described for the  $2H$  phases of TaS<sub>2</sub> and TaSe<sub>2</sub> crystals. To measure the susceptibility, we use a diamond anvil cell with a pressure transmitting medium of a methanol-ethanol mixture (4:1), which is considered to yield quasihydrostatic conditions up to the pressures of interest in our experiment [18,34]. Pressure was determined by the ruby fluorescence method [35]. We measure on small single crystalline samples cut into parallelepipeds of size about  $100 \times 100 \times 30$  μm<sup>3</sup>. The susceptibility is obtained by a conventional ac method using a transformer and a lock-in amplifier [18]. For the resistance we use a Bridgman pressure cell with steatite as the pressure transmitting medium [36]. Platinum wires were passed through the pyrophyllite gasket. Samples are cut into pieces of approximate size of  $\sim 100 \times 400 \times 60$  μm<sup>3</sup> and contacted to the platinum leads in the pressure cell. The temperature was controlled by a motor, gradually introducing the cell attached to a cane into the cryostat. The electrical resistance measurements were performed using a Keithley 220 source and a Keithley 2182 nanovoltmeter. Two samples were measured simultaneously, giving the same results. We could not appropriately determine the volume of samples or the geometrical factor. Thus, we provide relative temperature variations of susceptibility and resistance.

Figure 1 displays the susceptibility and resistance versus temperature curves obtained at different pressures at low temperatures. We determine  $T_c$  from the onset of the superconducting resistive and magnetic transition curves, defined as the intersection of two tangents, one to the flat portion of the curve above and the second to the steepest variation in the signal below the superconducting transition. In all cases we obtain sharp transitions, providing an unambiguous determination of the superconducting  $T_c$ . Sometimes we observe in the resistance measurements a small nonzero residual value in

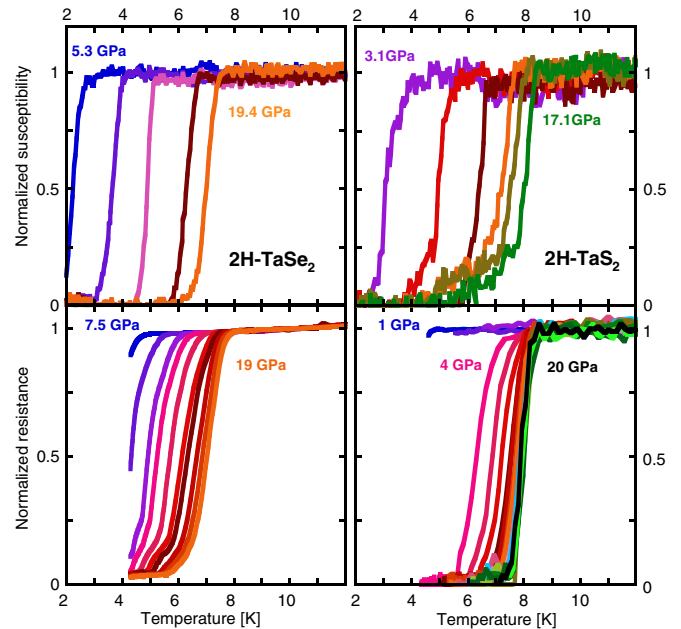


FIG. 1. Upper panels: Susceptibility of  $2H$ -TaSe<sub>2</sub> (left panel) and  $2H$ -TaS<sub>2</sub> (right panel) as a function of temperature for several applied pressures (5.3, 8.1, 11.7, 16.7, and 19.4 GPa for  $2H$ -TaSe<sub>2</sub> and 3.1, 5.8, 7.9, 9.8, 14.8, and 17.1 GPa for  $2H$ -TaS<sub>2</sub>). Susceptibility has been normalized to the value found at 10 K, and the low-temperature value has been modified to give zero. Lower panels: Resistance as a function of temperature for  $2H$ -TaSe<sub>2</sub> (left panel) and for  $2H$ -TaS<sub>2</sub> (right panel) for several applied pressures (from 7.5 to 15 by 1.5 GPa steps and then every GPa up to 19 GPa for  $2H$ -TaSe<sub>2</sub> and every GPa from 1 to 20 GPa for  $2H$ -TaS<sub>2</sub>). The resistance has been normalized to its value at 10 K.

the superconducting phase, which we attribute to two contacts touching each other at one side of the sample in the pressure cell. This does not influence the determination of  $T_c$ .

## III. RESULTS

The evolution of  $T_{CDW}$  under pressure was determined by calculating the temperature derivative of the resistance,  $dR(T)/dT$ , from the measured resistance versus temperature curves. In Fig. 2, we show  $dR(T)/dT$  for different pressures. The development of the CDW produces a gap on the Fermi surface that causes a sudden increase in the resistance which induces a downward peak in  $dR(T)/dT$  [37]. Their positions in the curves are signalled on Fig. 2 by small arrows. The obtained pressure dependence of  $T_c$  and  $T_{CDW}$  is shown in Fig. 3.

In  $2H$ -TaSe<sub>2</sub>, we find that pressure provokes an increase of  $T_c$ , with a slope of 0.58 K/GPa, between 2 and 8 GPa. The maximum is attained at  $T_c = 8.2$  K at a pressure of 23 GPa. On the other hand,  $T_{CDW}$ , which signals, as discussed above, an ICDW transition, decreases slowly to about 4 GPa. At 4 GPa we observe a jump. On further compression,  $T_{CDW}$  continues its rather slow decrease, reaching a value of  $\sim 90$  K at 20 GPa.

$2H$ -TaS<sub>2</sub> shows a similar behavior. We find an initial slope  $dT_c/dP = 1.05$  K/GPa below 6 GPa, which then slows down to 0.45 K/GPa, between 6 and 9.5 GPa. At low pressure,  $T_{CDW}$  decreases slowly, similarly to previous results [26]. At 4

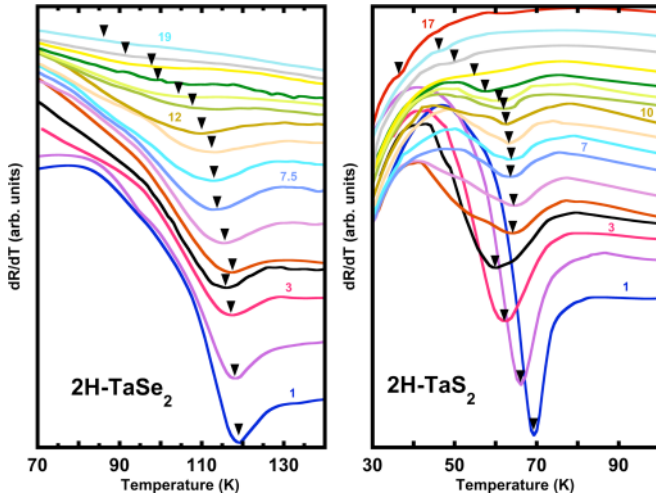


FIG. 2. Derivative of the resistance close to the CDW ordering temperature for respectively  $2H\text{-TaSe}_2$  (left panel) and  $2H\text{-TaS}_2$  (right panel) for different pressures [1, 2, 3, 4, 5, 6, 7.5, 9, 10.5, 12, 13.5, 15, 16, 17, 18, and 19 GPa (left) and every GPa from 1 to 17 GPa (right)]. Curves are shifted in the y axis for clarity. An arrow is used to mark the position where we take  $T_{CDW}$  to give the pressure dependence discussed in Fig. 3.

GPa we observe a sharp jump, similar to the one observed in  $2H\text{-TaSe}_2$ . Above the jump,  $T_{CDW}$  continues its slow decrease down to  $\sim 40$  K at 17 GPa.

#### IV. DISCUSSION AND CONCLUSIONS

Within the well-proven Bilbro-McMillan approach [38], the superconductivity (SC) involves the portions of carriers which are not gapped by CDW, explaining their mutual competition. In quasi-one-dimensional (1D) systems, CDWs are originated by strong nesting of the parallel Fermi surface (FS). Application of pressure destroys the CDW at a critical pressure  $P_c$ , where  $T_c$  attains its maximum value [39–42]. While the loss of Fermi-surface portions due to nesting dominates the interplay between CDW and superconductivity in quasi-1D systems, the situation is more involved in quasi-2D systems. Due to the quasicylindrical nature of the 2D FSs, the nesting anomalies are much weaker [43] and then electron-phonon ( $e$ -ph) coupling is more important in creating CDWs than in quasi-1D systems [30,44–48]. The interplay between competing electronic and elastic degrees of freedom produces then minima in the free energy landscape that easily favor different kinds of CDWs (commensurate or incommensurate) when modifying pressure and temperature.

For  $2H\text{-TaSe}_2$ , the jump in  $T_{CDW}$  observed at about 4 GPa agrees with the previously reported pressure-induced lock-in transition into a CCDW [28] (right green line in Fig. 3). Such a peak in the variation of density-wave transition temperatures with pressure has been observed in other materials [49,50] and has been unequivocally ascribed to transitions from an incommensurate to a commensurate state. McMillan explained the first-order nature of the incommensurate/commensurate transition temperature driven by a Ginzburg-Landau analysis [51]. By analogy, we expect that the pressure-driven

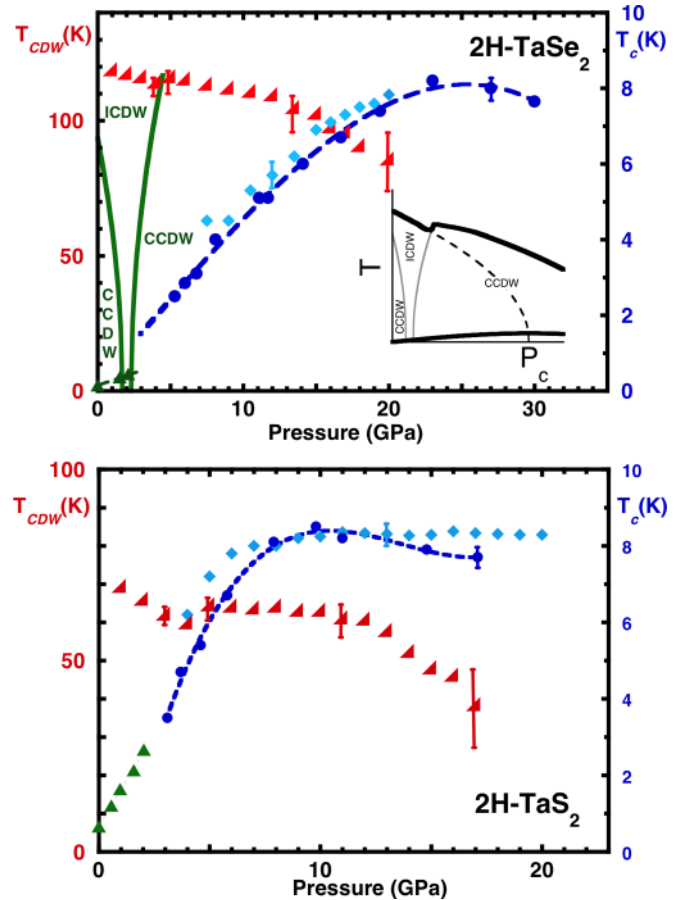


FIG. 3. Phase diagram of the superconducting transition obtained from susceptibility (blue solid circles), resistance (light blue lozenges), and of the CDW transition (red triangles). Solid triangles at low pressures have been obtained from Smith *et al.* [25]. Typical error bars are shown. Blue lines are guides to the eyes. Green dashed lines in the top panel are the positions of the CDW as found in previous works for  $2H\text{-TaSe}_2$  [26,28,29]. Inset: Proposed phase diagram for both compounds. Black dashed lines are extrapolations of the low-pressure range data (see text).

incommensurate/commensurate transition is also a first-order transition and induce a jump in the  $T_{CDW}(P)$  phase diagram.

The behavior at ambient pressure for both compounds is similar. At high temperatures they show a transition into an ICDW, with a lock-in transition to a CCDW at lower temperatures [27,28,52]. We can then speculate that the jumps around 4 GPa in both  $2H\text{-TaSe}_2$  and  $2H\text{-TaS}_2$  are due to the same phenomenon. That would imply that the ICDW in  $2H\text{-TaS}_2$  locks to the lattice with increasing pressure. We include this possibility in the proposed general phase diagram shown in the inset of Fig. 3.

The weak pressure dependence of  $T_{CDW}$  at higher pressures indicates, on the other hand, that the CDW in this pressure range is remarkably robust to a reduction of the lattice parameters. This is not possible to explain within a pure nesting scenario, because the band structure and the nesting condition are extremely sensitive to pressure. On other hand, in the simplest lattice scenario through an  $e$ -ph coupling, theories

have to reconcile the absence of pressure dependence of  $T_{\text{CDW}}$  with the phonon hardening due to pressure.

It is interesting to discuss a recent model proposed to explain the CDW in  $2H$  transition metal dichalcogenides [53]. It considers that the CDW transition takes the form of a phase transition in a system of interacting Ising pseudospins. These can be associated to the six transition metal atoms lying on the vertices of the in-plane hexagon described in Ref. [45]. These might have a tendency to cluster in such a way as to form an inverse star towards the transition metal atom at the center of the hexagon. This type of distortion has an intrinsic degeneracy locally, i.e., the transition metal atoms can choose between two inverse stars with the same type of displacement. By analogy with an up and down Ising ferromagnet, this is called an Ising pseudospin model. Thus, order is only short ranged and the development of a macroscopic static distortion corresponds to an ordering of the Ising pseudospins [54]. This order-disorder transition is characterized by the absence of unstable zero energy phonon softening at the transition, as is confirmed by the reported nonzero soft mode for  $2H$ -TaSe<sub>2</sub> [55]. Furthermore, the idea of preexisting disordered deformations stems from the observation of a gap that is five times larger than expected from the weak-coupling formula [56] and could be used to explain the robustness of the CDW at higher pressures. It would imply, though, that the model describes better the transition metal dichalcogenides with large interlayer separations,  $2H$ -TaSe<sub>2</sub> and  $2H$ -TaS<sub>2</sub>, than  $2H$ -NbSe<sub>2</sub>. In the latter compound, the CDW has a lower critical temperature (30 K) and disappears already at 5 GPa [12,14].

Regarding the superconductivity, our measurements show that  $T_c$  is strongly enhanced within the commensurate high-pressure CDW phase. The increase in  $T_c$  might be a consequence of phonon hardening or of Fermi-surface-induced changes with pressure. But it is not straightforward to think of a scenario where such features act on superconductivity independently of the CDW. A possibility is that both phenomena involve widely different parts of the Fermi surface associated with the absence of or small interband correlations.

It is interesting to note that the extrapolation of the low-pressure (below the jump) behavior of the ICDW up to higher pressures using a mean field approach  $T_{\text{ICDW}} = T_{\text{ICDW}}^0 \sqrt{\frac{P_c - P}{P_c}}$  (where  $T_{\text{ICDW}}^0$  is the ambient pressure ICDW transition) leads to values for  $T_{\text{ICDW}}^0$  becoming zero at a pressure  $P_c$  roughly when the  $T_c(P)$  curve ceases to increase in both materials. In the past, a mean field power law has been used for the low-pressure commensurate transition in

$2H$ -TaSe<sub>2</sub> [29,57]. We have tentatively highlighted this aspect in the inset of Fig. 3. Although the extrapolation is, of course, connected with very large errors, it invites the speculation that there might be a mutually exclusive relation between incommensurate CDW and superconductivity. Note, however, that the Bilbro-McMillan approach discussed above in relation with the competition between incommensurate CDW and superconductivity no longer applies when the incommensurate CDW has passed a transition into a commensurate CDW.

It is worth noting that the phase diagrams of  $2H$  Ta-based dichalcogenides are in sharp contrast from those of other transition metal dichalcogenides such as  $1T$ -TiSe<sub>2</sub>, where superconductivity is observed at the vicinity of the pressure range of ICDW [17,58], or  $2H$ -NbSe<sub>2</sub>, where  $T_c$  is only moderately affected by the pressure [12,18]. In this last compound, the insensitivity of the superconducting critical temperature to the CDW transition is due to the fact that high-energy optical phonon modes strongly contribute to the Eliashberg function, whereas the low-energy longitudinal acoustic mode that drives the CDW transition barely contributes to superconductivity [59].

We conclude that understanding the value of  $T_c$  in layered materials requires studying modifications of the band structure, phonon dispersion, and electron phonon coupling. Here we have shown that  $T_c$  can considerably increase within a CDW, by more than an order of magnitude.

#### ACKNOWLEDGMENTS

We acknowledge discussions with P. Grigoriev, R. Wehrt, N. Lera, and J. V. Alvarez. D.C.F. gratefully acknowledges support from the Brazilian agencies CAPES and CNPq. This work was partially supported by the French National Research Agency through the project Subrissyme ANR-12-JS04-0003-01 and by the Spanish MINECO (FIS2014-54498-R, MAT-2014-56143-R, MDM-2014-0377, and MDM-2015-0538), by the Comunidad de Madrid through program Nanofrontmag, and by the European Union (Graphene Flagship Contract No. CNECT-ICT-604391 and COST MP1201 action). The susceptibility versus temperature data at high pressures, where the strong increase in  $T_c$  was first noticed, were taken by the late V. G. Tissen of the Institute of Solid State Physics, Chernogolovka, Russia, during his sabbatical stay in Madrid, which was financed by MINECO. We also acknowledge the technical support of UAM's workshops, SEGAINVEX.

- 
- [1] B. M. Ludbrook, G. Levy, P. Nigge, M. Zonno, M. Schneider, D. J. Dvorak, C. N. Veenstra, S. Zhdanovich, D. Wong, P. Dosanjh, C. Straer, A. Stöhr, S. Forti, C. R. Ast, U. Starke, and A. Damascelli, Evidence for superconductivity in Li-decorated monolayer graphene, *Proc. Natl. Acad. Sci. USA* **112**, 11795 (2015).
- [2] J. Chapman, Y. Su, C. A. Howard, D. Kundys, A. N. Grigorenko, F. Guinea, A. K. Geim, I. V. Grigorieva, and R. R. Nair, Superconductivity in Ca-doped graphene, *Sci. Rep.* **6**, 23254 (2016).
- [3] J. M. Lu, O. Zheliuk, I. Leermakers, N. F. Q. Yuan, U. Zeitler, K. T. Law, and J. T. Ye, Evidence for two-dimensional Ising superconductivity in gated MoS<sub>2</sub>, *Science* **350**, 1353 (2015).
- [4] H. Suderow, Opening the gate on superconductivity, *Science* **350**, 1316 (2015).
- [5] X. Xi, Z. Wang, W. Zhao, J.-H. Park, K. T. Law, H. Berger, and L. Forro, J. Shan, and K. F. Mak, Ising pairing in superconducting NbSe<sub>2</sub> atomic layers, *Nat. Phys.* **12**, 139 (2015).

- [6] M. S. El-Bana, D. Wolverson, S. Russo, G. Balakrishnan, D. MckPaul, and S. J. Bending, Superconductivity in two-dimensional NbSe<sub>2</sub> field effect transistors, *Supercond. Sci. Technol.* **26**, 125020 (2013).
- [7] Y. Cao, A. Mishchenko, G. L. Yu, E. Khestanova, A. P. Rooney, E. Prestat, A. V. Kretinin, P. Blake, M. B. Shalom, C. Woods, J. Chapman, G. Balakrishnan, I. V. Grigorieva, K. S. Novoselov, B. A. Piot, M. Potemski, K. Watanabe, T. Taniguchi, S. J. Haigh, A. K. Geim, and R. V. Gorbachev, Quality heterostructures from two-dimensional crystals unstable in air by their assembly in inert atmosphere, *Nano Lett.* **15**, 4914 (2015).
- [8] E. Navarro-Moratalla, J. Island, S. Mañas-Valero, E. Pinilla-Cienfuegos, A. Castellanos-Gómez, J. Quereda, G. Rubio-Bollinger, L. Chirolli, J. A. Silva Guillen, N. Agrait, G. A. Steele, F. Guinea, H. van der Zant, and E. Coronado, Enhanced superconductivity in atomically-thin TaS<sub>2</sub> layers, *Nature Commun.* **7**, 11043 (2016).
- [9] J. A. Galvis, P. Rodière, I. Guillamón, M. R. Osorio, J. G. Rodrigo, L. Cario, E. Navarro-Moratalla, E. Coronado, S. Vieira, and H. Suderow, Scanning tunneling measurements of layers of superconducting 2H-TaSe<sub>2</sub>: Evidence for a zero-bias anomaly in single layers, *Phys. Rev. B* **87**, 094502 (2013).
- [10] J. A. Galvis, L. Chirolli, I. Guillamón, S. Vieira, E. Navarro-Moratalla, E. Coronado, H. Suderow, and F. Guinea, Zero-bias conductance peak in detached flakes of superconducting 2H-TaS<sub>2</sub> probed by scanning tunneling spectroscopy, *Phys. Rev. B* **89**, 224512 (2014).
- [11] J. A. Wilson, F. J. Disalvo, and S. Mahajan, Charge-density waves and superlattices in the metallic layered transition metal dichalcogenides, *Adv. Phys.* **24**, 117 (1975).
- [12] C. Berthier, P. Molinié, and D. Jérôme, Evidence for a connection between charge density waves and the pressure enhancement of superconductivity in 2H-NbSe<sub>2</sub>, *Solid State Commun.* **18**, 1393 (1976).
- [13] E. Coronado, C. Martí-Gastaldo, E. Navarro-Moratalla, A. Ribera, S. Blundell, and P. Bajer, Coexistence of superconductivity and magnetism by chemical design, *Nat. Chem.* **2**, 1031 (2010).
- [14] Y. Feng, J. Wang, R. Jaramillo, J. van Wezel, S. Haravifard, G. Srajer, Y. Liu, Z.-A. Xu, P. B. Littlewood, and T. F. Rosenbaum, Order parameter fluctuations at a buried quantum critical point, *Proc. Natl. Acad. Sci. USA* **109**, 7224 (2012).
- [15] E. Morosan, H. Zandbergen, B. Dennis, J. Boas, Y. Onose, T. Klimczuk, A. Ramírez, N. Ong, and R. Cava, Superconductivity in Cu<sub>x</sub>TiSe<sub>2</sub>, *Nat. Phys.* **2**, 544 (2006).
- [16] B. Sipoš, A. F. Kusmartseva, A. Akrap, H. Berger, L. Forró, and E. Tutiš, From Mott state to superconductivity in 1T-TaS<sub>2</sub>, *Nat. Mater.* **7**, 960 (2008).
- [17] A. F. Kusmartseva, B. Sipoš, H. Berger, L. Forró, and E. Tutiš, Pressure Induced Superconductivity in Pristine 1T-TiSe<sub>2</sub>, *Phys. Rev. Lett.* **103**, 236401 (2009).
- [18] H. Suderow, V. G. Tissen, J. P. Brison, J. L. Martínez, and S. Vieira, Pressure Induced Effects on the Fermi Surface of Superconducting 2H-NbSe<sub>2</sub>, *Phys. Rev. Lett.* **95**, 117006 (2005).
- [19] R. A. Klemm, *Layered Superconductors* (Oxford University Press, Oxford, U.K., 2012).
- [20] A. H. Castro Neto, Charge Density Wave, Superconductivity, and Anomalous Metallic Behavior in 2D Transition Metal Dichalcogenides, *Phys. Rev. Lett.* **86**, 4382 (2001).
- [21] I. Guillamon, H. Suderow, S. Vieira, L. Cario, P. Diener, and P. Rodiere, Superconducting Density of States and Vortex Cores of 2H-NbSe<sub>2</sub>, *Phys. Rev. Lett.* **101**, 166407 (2008).
- [22] Y. Yokoya, T. Kiss, A. Chainani, S. Shin, M. Nohara, and H. Takagi, Fermi surface sheet-dependent superconductivity in 2H-NbSe<sub>2</sub>, *Science* **294**, 2518 (2001).
- [23] D. J. Rahn, S. Hellmann, M. Kallane, C. Sohr, T. K. Kim, L. Kipp, and K. Rossnagel, Gaps and kinks in the electronic structure of the superconductor 2H-NbSe<sub>2</sub> from angle resolved photoemission at 1 K, *Phys. Rev. B* **85**, 224532 (2012).
- [24] B. Keimer, S. A. Kivelson, M. R. Norman, S. Uchida, and J. Zaanen, From quantum matter to high-temperature superconductivity in copper oxides, *Nature (London)* **518**, 179 (2015).
- [25] T. F. Smith, R. N. Shelton, and R. E. Schwall, Superconductivity of TaS<sub>2-x</sub>Se<sub>x</sub> layer compounds at high pressure, *J. Phys. F: Met. Phys.* **5**, 1713 (1975).
- [26] R. Delaplace, P. Molinié, and D. Jérôme, On the pressure dependence of a charge density wave state in 2H-TaS<sub>2</sub>, *J. Phys. Lett.* **37**, 13 (1976).
- [27] G. Scholz, O. Singh, R. Frindt, and A. Curzon, Charge density wave commensurability in 2H-TaS<sub>2</sub> and Ag<sub>x</sub>TaS<sub>2</sub>, *Solid State Commun.* **44**, 1455 (1982).
- [28] D. B. McWhan, R. M. Fleming, D. E. Moncton, and F. J. DiSalvo, Reentrant Lock-in Transition of the Charge-Density Wave in 2H-TaSe<sub>2</sub> at High Pressure, *Phys. Rev. Lett.* **45**, 269 (1980).
- [29] C. Chu, L. Testardi, F. DiSalvo, and D. Moncton, Pressure effects on the charge-density-wave phases in 2H-TaSe<sub>2</sub>, *Phys. Rev. B* **14**, 464 (1976).
- [30] L. Bulaevskii, Structural transitions with formation of charge-density waves in layer compounds, *Sov. Phys. Usp.* **19**, 836 (1976).
- [31] P. B. Littlewood and T. M. Rice, Theory of the Splitting of Discommensurations in the Charge-Density-Wave State of 2H-TaSe<sub>2</sub>, *Phys. Rev. Lett.* **48**, 27 (1982).
- [32] T. M. Rice, Landau theory of the charge-density-wave state in tantalum diselenide under pressure, *Phys. Rev. B* **23**, 2413 (1981).
- [33] M. Steinitz and J. Genossar, Anharmonicity, anisotropy, inter-layer coupling and the reentrant lock-in transition in 2H-TaSe<sub>2</sub>, *J. Phys. C: Solid State Phys.* **14**, L939 (1981).
- [34] N. Tateiwa and Y. Haga, Appropriate pressure-transmitting media for cryogenic experiment in the diamond anvil cell up to 10 GPa, *J. Phys.: Conf. Ser.* **215**, 012178 (2010).
- [35] P. D. Horn and Y. M. Gupta, Luminescence R-line spectrum of ruby crystals shocked to 125 kbar along the crystal *c* axis, *Phys. Rev. B* **39**, 973 (1989).
- [36] G. Garbarino and M. Núñez-Regueiro, Pressure and the quadratic temperature term in the electrical resistance of NbTi, *Solid State Commun.* **142**, 306 (2007).
- [37] P. M. Horn and D. Guidotti, Critical behavior at electronically driven structural transitions in anisotropic metals, *Phys. Rev. B* **16**, 491 (1977).

- [38] G. Bilbro and W. L. McMillan, Theoretical model of superconductivity and the martensitic transformation in A15 compounds, *Phys. Rev. B* **14**, 1887 (1976).
- [39] P. Monceau, Electronic crystals: an experimental overview, *Adv. Phys.* **61**, 325 (2012).
- [40] M. Núñez Regueiro, J.-M. Mignot, and D. Castello, Superconductivity at high pressure in NbSe<sub>3</sub>, *Europhys. Lett.* **18**, 53 (1992).
- [41] M. Núñez Regueiro, J.-M. Mignot, M. Jaime, D. Castello, and P. Monceau, Superconductivity under pressure in linear chalcogenides, *Synth. Met.* **56**, 2653 (1993).
- [42] M. Monteverde, J. Lorenzana, P. Monceau, and M. Núñez-Regueiro, Quantum critical point and superconducting dome in the pressure phase diagram of *o*-TaS<sub>3</sub>, *Phys. Rev. B* **88**, 180504(R) (2013).
- [43] K. Rossnagel, O. Seifarth, L. Kipp, M. Skibowski, D. Voß, P. Krüger, A. Mazur, and J. Pollmann, Fermi surface of 2*H*-NbSe<sub>2</sub> and its implications on the charge-density-wave mechanism, *Phys. Rev. B* **64**, 235119 (2001).
- [44] R. V. Coleman, B. Giambattista, P. K. Hansma, A. Johnson, W. W. McNairy, and C. G. Slough, Direct observation of a surface charge density wave, *Adv. Phys.* **37**, 559 (1988).
- [45] K. Rossnagel, On the origin of charge-density waves in select layered transition-metal dichalcogenides, *J. Phys.: Condens. Matter* **23**, 213001 (2011).
- [46] T. Rice and G. Scott, New Mechanism for a Charge-Density-Wave Instability, *Phys. Rev. Lett.* **35**, 120 (1975).
- [47] M. D. Johannes, I. I. Mazin, and C. A. Howells, Fermi-surface nesting and the origin of the charge-density wave in NbSe<sub>2</sub>, *Phys. Rev. B* **73**, 205102 (2006).
- [48] M. D. Johannes and I. I. Mazin, Fermi-surface nesting and the origin of the charge-density wave in NbSe<sub>2</sub>, *Phys. Rev. B* **77**, 165135 (2008).
- [49] B. J. Klemme, S. E. Brown, P. Wzietek, G. Kriza, P. Batail, D. Jérôme, and J. M. Fabre, Commensurate and incommensurate spin-density waves and a modified phase diagram of the Bechgaard salts, *Phys. Rev. Lett.* **75**, 2408 (1995).
- [50] W. Kaddour, P. Auban-Senzier, H. Raffy, M. M. Monteverde, J.-P. Pouget, C. R. Pasquier, P. Alemany, E. Canadell and L. Vallade, Charge density wave and metallic state coexistence in the multiband conductor TTF[Ni(dmit)<sub>2</sub>]<sub>2</sub>, *Phys. Rev. B* **90**, 205132 (2014).
- [51] W. L. McMillan, Microscopic model of charge-density waves in 2*H*-TaSe<sub>2</sub>, *Phys. Rev. B* **16**, 643 (1977).
- [52] H. Nishihara, G. A. Scholz, M. Naito, R. F. Frindt, and S. Tanaka, NMR of <sup>181</sup>Ta in 2*H*-TaS<sub>2</sub> and 2*H*-TaSe<sub>2</sub>—observation of locally commensurate CDW, *J. Magn. Magn. Mater.* **31-34**, 717 (1983).
- [53] L. P. Gorkov, Strong electron-lattice coupling as the mechanism behind charge density wave transformations in transition-metal dichalcogenides, *Phys. Rev. B* **85**, 165142 (2012).
- [54] M. D. Núñez-Regueiro, J. M. Lopez-Castillo, and C. Ayache, Thermal conductivity of 1*T*-TaS<sub>2</sub> and 2*H*-TaSe<sub>2</sub>, *Phys. Rev. Lett.* **55**, 1931 (1985).
- [55] D. E. Moncton, J. D. Axe, and F. J. DiSalvo, Neutron scattering study of the charge-density wave transitions in 2*H*-TaSe<sub>2</sub> and 2*H*-NbSe<sub>2</sub>, *Phys. Rev. B* **16**, 801 (1977).
- [56] A. S. Barker, Jr., J. A. Ditzenberger, and F. J. DiSalvo, Infrared study of the electronic instabilities in tantalum disulfide and tantalum diselenide, *Phys. Rev. B* **12**, 2049 (1975).
- [57] D. C. Freitas, P. Rodière, M. Núñez, G. Garbarino, A. Sulpice, J. Marcus, F. Gay, M. A. Continentino, and M. Núñez-Regueiro, Experimental consequences of quantum critical points at high temperatures, *Phys. Rev. B* **92**, 205123 (2015).
- [58] Y. I. Joe, X. M. Chen, P. Ghaemi, K. D. Finkelstein, G. A. de la Pea, Y. Gan, J. C. T. Lee, S. Yuan, J. Geck, G. J. MacDougall, T. C. Chiang, S. L. Cooper, E. Fradkin, and P. Abbamonte, Emergence of charge density wave domain walls above the superconducting dome in 1*T*-TiSe<sub>2</sub>, *Nat. Phys.* **10**, 421 (2014).
- [59] M. Leroux, I. Errea, M. Le Tacon, S. M. Souliou, G. Garbarino, L. Cario, A. Bosak, F. Mauri, M. Calandra, and P. Rodière, Strong anharmonicity induces quantum melting of charge density wave in 2*H*-NbSe<sub>2</sub> under pressure, *Phys. Rev. B* **92**, 140303(R) (2015).